Title:

Highly Selective Artificial Cholesteryl Crown Ether K+-Channels

Zhanhu Sun,[1] Mihail Barboiu,[1,*] Yves-Marie Legrand,[1] Eddy Petit,[1] Alexandru Rotaru[2]

[1]Adaptive Supramolecular Nanosystems Group, Institut Europeen des Membranes, ENSCM-UM-CNRS UMR-5635 Place E. Bataillon, CC 047, F-34095, Montpellier Cedex 5 (France)

[2]Petru Poni Institute of Macromolecular Chemistry of Romanian Academy 41A Aleea Gr. Ghica Voda, Iasi (Romania)

*E-mail: mihail-dumitru.barboiu@univ-montp2.fr

Abstract

The bacterial KcsA channel conducts K^+ cations at high rates while excluding Na^+ cations. Herein, we report an artificial ion-channel formed by H-bonded stacks of crown-ethers, where K^+ cation conduction is highly preferred to Na^+ cations. The macrocycles aligned along the central pore surround the K^+ cations in a similar manner to the water around the hydrated cation, compensating for the energetic cost of their dehydration. In contrast, the Na^+ cation does not fit the macrocyclic binding sites, so its dehydration is not completely compensated. The present highly K^+-selective macrocyclic channel may be regarded as a biomimetic of the KcsA channel.

The exchange of ions across the lipid bilayer membrane is a prerequisite for many physiological processes.[1,2] Natural ion channels play significant roles in supporting the metabolism of living cells, and their dysfunction can lead to a number of diseases, even death.[3] Among ion channels, the KcsA K^+ channel is highly selective for K^+ cations. It has a hydrophobic conical pore and the selectivity filter in the middle, affording closely spaced carbonyl sites for the selective coordination of the dehydrated K^+ cations.[4]

Biomimetic approaches have been used to develop artificial supramolecular channels with the hope to reach the high selectivity of the KcsA channel.[5–7] Barrel-stave systems,[8] G-quadruplex,[9] lariat crown ethers,[10] hydraphiles[11] or peptide-appended crownethers[12,13] have been intensively used to construct ion-channels for selective ionic translocation. We are interested in the possibility to self-organize heteroditopic ureido crown ethers through H-bonding for suitable membrane ion channel transport functions.[14] This approach has been extended to light-responsive channels, and the structure-activity relationships have been determined.[15] We know from our previous studies, that lipophilic ureido crown ethers disrupt the bilayer membrane at low concentration, showing rare single channel openings. At higher concentration, a rich array of interconverting channel conductance states are observed for K^+ cations. The channels arise from H-bonded stacks of crown ethers where transport of cations would occur by the macrocycles around a central large pore.[14b] Within this context we presumed that the entropic cost of cation binding/transport must be far larger than the case where these macrocyclic receptors present a restricted conformational entropy in the bilayer. Their self-assembly can influence their dynamic distribution and the stability of the channels within the bilayer membrane. Within this context, steroids are important cyclic compounds,[16] intensively used in the construction and stabilization of many ion channel superstructures.[16–18] Based on these observations, we designed and prepared in this study, a series of cholesteryl-thioureido-ethylamide crown ethers that self-assemble into robust ion-channels and show a remarkably high selectivity for the K^+ against Na^+ cations, close to that of natural channels. The thioureido-ethylamide linker connecting crown ether and cholesterol moieties form H-bonded arrays of channel-type stacks of crown ethers disposed in very close proximity pointing towards the center of the channel and expected to serve as ion selectivity filters.[19] Cholesterol moieties aiming to stabilize the channels, act as anchoring arms inducing low diffusivity, clustering, and higher preorganization of the macrocycles in lipid bilayers.[20]

The synthesis of key compounds **1a-c** is presented in Scheme1. 3β-Cholest-5-en-3-yl-N-(2-aminoethyl) carbamate **2** was prepared according to the literature[21] and then converted to 3β-cholest-5-en-3-yl-N-(2-isothiocyanatoethyl)-carbamate,[22] which was reacted in situ with the corresponding 4-amino-benzo-crown-ethers **3a/3b**, to provide cholesteryl-thioureido-ethylamide crown ethers **1a** and **1b**. The macrocyclic heads are benzo-15-crown-5 in **1a** and benzo-18-crown-6 in **1b**, known to be dimensionally compatible with Na^+ and K^+ cations, respectively. Compound **1c** was prepared from N-Boc-1,2-ethylenediamine and 4′-isothiocyanatobenzo-15-crown-5. All compounds display spectroscopic and analytical data in accordance with their structures (Supporting Information, Figures S1-S6).
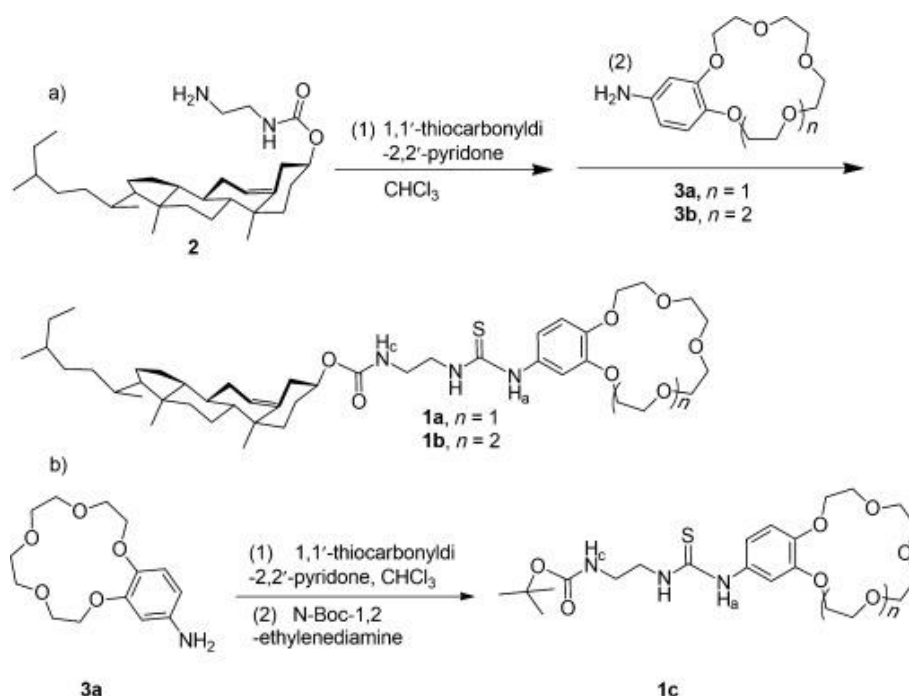
Scheme 1. Synthesis of a) cholesteryl thioureidoethylamide-15-crown-5-ether **1a**, and cholesteryl thioureidoethylamide-18-crown-6-ether **1b** and b) of the reference tert-butylthioureidoethylamide-15-crown-5 ether, **1c**.

The self-assembly behaviors in solution were investigated by ^{1}H NMR dilution experiments. Amazingly, the chemical shift of H_a of the thiourea group of compound **1a** shows at low concentration (9 mM) an unexpected chemical shift at 8.0 ppm (Figure 1a), reflecting its intramolecular H-bonding in the monomer. Then, the upfield H_a chemical shifts until 7.83 ppm (C_{1a}=21 mM) toward a plateau (C_{1a}=21-43 mM) and then above 43 mM, the H_a signal shifts gradually from 7.83 ppm to lower field. Rather, the plateau associated with the constant upfield shift of H_c in the carbamate moiety (Figure 1b) indicates a stepwise association process to form at least two distinct types of aggregates. We assume that the

process occurring at the plateau concentrations is the formation of a dimer from monomers. Then, the dimer would be essentially fully formed below 43 mM, when oligomeric species emerge. This behavior is similar with that of previously reported ureido crown ethers,[14b] consistent with the formation of a range of oligomers beyond the dimer since these species would give a steady change over the concentration range. Similar behaviors were observed for compounds **1b** and **1c** (Supporting Information, Figures S7, S8). Meanwhile, structural information on the self-association of **1a-c** in solid state was obtained using atomic force microscopy (AFM). The compounds **1a** and **1b** form thin films from CHCl$_3$ (thickness of ca. 100 nm), with circular and boat-shape nanometric holes, respectively (Supporting Information, Figures S9, S10). Presumably, the holes are the result of the amphiphilic self-assembly of the hydrophobic cholesteryl and the polar crown ether moieties, including intermolecular H-bonding and solvophobic effects. Importantly, in the absence of the bulky non-polar cholesteryl moiety, no uniform structures were obtained for compound **1c**, (data not shown), emphasizing the role of cholesterol to promote channel-like architectures.
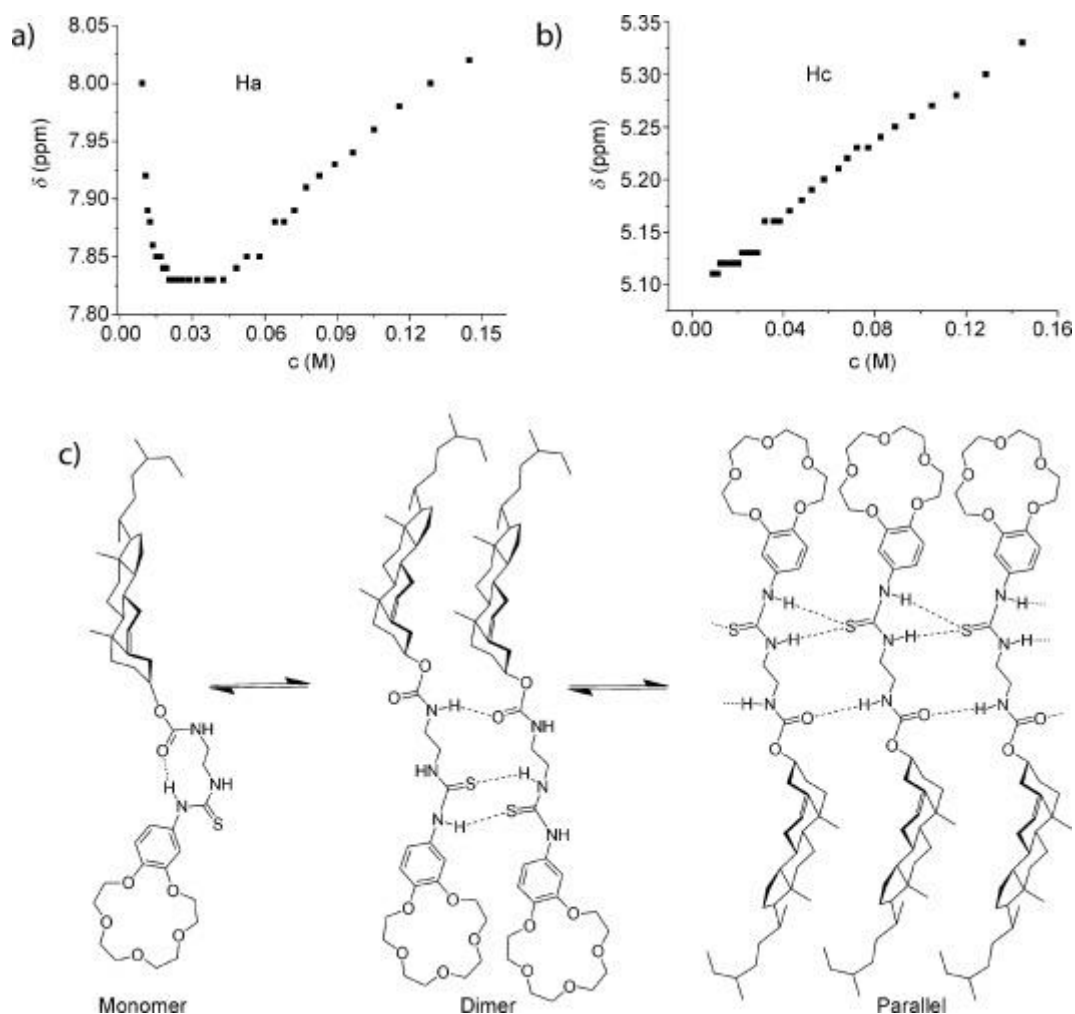
Figure 1. Chemical shifts of the a) N-Ha and b) N-H$_c$ protons plotted against the concentration of **1a** in CDCl$_3$ at 293 K. c) Concentration-dependent equilibria between intramolecularly H-bonded monomer, and intermolecularly H-bonded dimer and oligomers.

The transport activity of **1a,b**, dispersed within the L-α-phosphatidyl-choline before the formation of large unilamellar vesicles (LUV), towards alkali cations was evaluated using pH gradient assays.[23, 24] The results showed that **1a** is completely inactive towards Li$^+$, Na$^+$, and Cs$^+$ cations (Figure 2a; Supporting Information, Figures S14, S15, S18). Interestingly, **1a** is highly active towards K$^+$ cations and slightly active for Rb$^+$ cations. Figure **2c** illustrates the compound relative transport activity towards the different cations, which clearly emphasizes the selectivity of **1a** for K$^+$ and the good efficiency of **1b** for Rb$^+$ and Cs$^+$, especially compared to **1c**, which can be considered as inactive. The Hill analysis of K$^+$ transport through **1a** channels reveals a linear concentration-activity relationship with a Hill coefficient of 1.12 ± 0.08 ($R^2=0.922$), resembling that of a Class I channel.[25] The transport activity of **1a** decreased in the following order: K$^+$>Rb$^+$>Li$^+$≈Na$^+$≈Cs$^+$ (Table 1), corresponding to the Eisenman sequence IV or V.[26] We know from previously reported X-ray single-crystal structures, that lipophilic ureido-benzo-15-crown-5-ether and ureido-benzo-18-crown-6-ether bind Na$^+$ (Figure 3a) and K$^+$ (Figure 3b) cations, respectively, through one macrocycle, while a sandwich-type geometry has been determined for complexation of the bigger K$^+$ cations by two 15-crown-5-ethers moieties (Figure 3c).[27] The highly selective transport rate of K$^+$ cations is in part due to its sandwich-type recognition by the crown-ethers as observed in the crystal structure, completely surrounding the K$^+$ cations in a similar manner to the water molecules around the hydrated cation (Figure 3c, bottom).
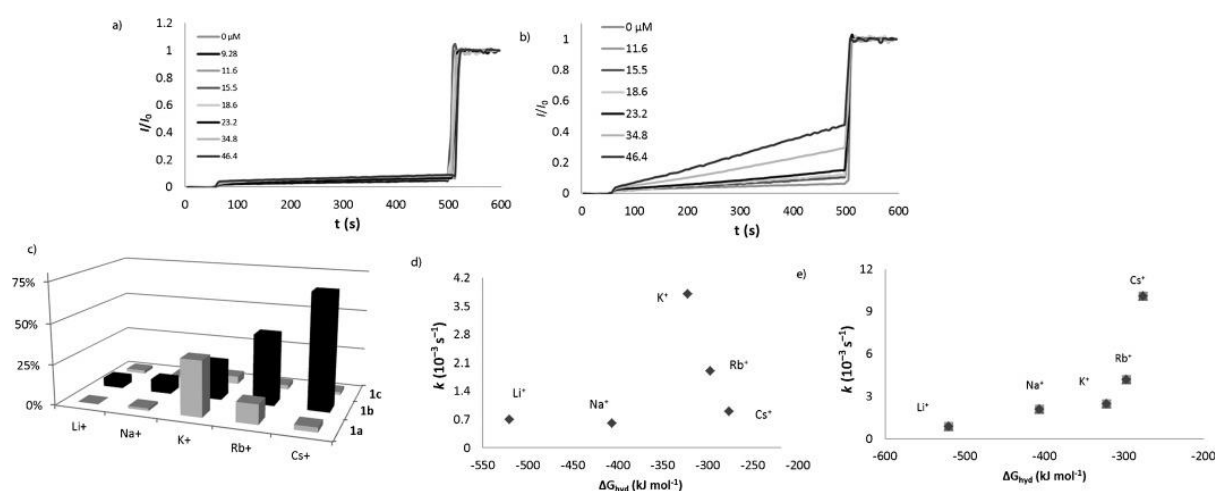
Figure 2. Transport of a) Na^+ and b) K^+ cations as determined in a pH gradient assay as a function of 1 a concentration. c) Transport percentage of alkali cations through LUVs containing 1:10 mol:mol, compd:lipid of **1a**, **1b**, and **1c**. Pseudo first-order rate constants k for the transport of alkali cations through LUVs containing d) **1a**: or e) **1b** compounds, k was calculated by calibration of fluorescence intensity ratio change to vesicle internal pH following a method previously demonstrated by Davis and co-workers.[24]
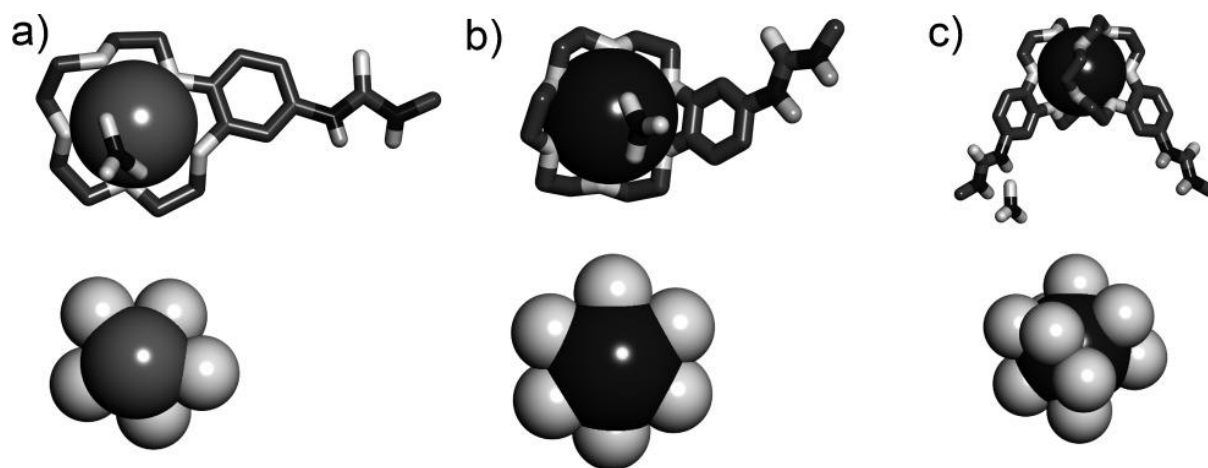

Figure 3. (top) X-ray crystal structures of a) ureido-benzo-15-crown-5-ether·$NaNO_3$; b) ureido-benzo-18-crown-6-ether·KNO_3 and ureido-benzo-15-crown-5-ether ·KNO_3 complexes. (bottom) Geometry of the oxygen atoms (white spheres) binding around Na^+ cations (left, grey spheres) and K^+ cations (middle and right, black spheres) in the presented X-ray crystal structures.[27]

Table 1. Transport EC_{50} and Hill factors of **1a-c** towards alkali cations

Comp.		Li+	Na+	K+	Rb+	Cs+
1a	EC_{50} [µM] Hill no.	–[a]	–[a]	26.5 1.12	31.4 0.55	–[a]
1b	EC_{50} [µM] Hill no.	–[a]	–[a]	29.1 0.49	26.4 0.72	25.1 1.10
1c	EC_{50} [µM] Hill no.	–[a]	–[a]	94.6 0.43	90.0 0.48	–[a]

[a]no activity detected.

In contrast, for the Na^+ cations, the macrocyclic binding sites are not covering the hydration sites, so Na^+ dehydration is not completely compensated (Figure 3a,b bottom). This is similar to how the KcsA K^+ channel functions, where the perfect positioning of the carbonyl moieties replacing the hydration sphere of K^+ cations in the active gate is determinant for the selective K^+ translocation against the imperfectly coordinated Na^+ cations. The exact transport mechanism is difficult to be completely described by these data, but the selective K^+-file permeation can be performed by successive coordination processes

along the parallel oriented crown channels acting as an exceptional lubricant in the hydrophilic part of the channel. This assumption is confirmed by the lower activity of **1b** towards Li^+, Na^+, and K^+ than Cs^+ and Rb^+ cations. **1b** is dimensionally compatible with K^+ cations, fitting the 18-crown-6-ether cavity, and forming the sandwich type complexes with Rb^+ and Cs^+, which are better complexed within the channel. The transport activity of **1b** decreases in the order of $Cs^+>Rb^+>K^+>Na^+≈Li^+$ (Table 1), that is, the Eisenman sequence I, corresponding also to the energetic penalty for ion dehydration.[26]

Finally, the control compound **1c** shows extremely low activities towards all cations (Table 1), confirming the significant anchoring role of cholesterol moiety stabilizing the ion-channel superstructures within the membrane. The EC_{50} values (the concentration in μM required to obtain 50% ion conduction) reveal that the presence of the cholesteryl moiety in **1a,b** has increased the transport activity by more than three times than **1c**.

In conclusion, the high selectivity of K^+ transport through the artificial cholesteryl-thioureido crown ether ion channels 1 a shows formal similarity with that of the KcsA K^+ channel. The biological K^+ channel has a selectivity filter in the middle of the channel, affording closely spaced carbonyl sites for the perfect coordination the K^+ cations.[4]

We know that cholesteryl compounds form liquid crystalline phases, and the textures revealed by AFM suggest that might the case with these derivatives. The self-assembly of ion channels **1a** in the bilayer is probably stabilized by the cholesterol moieties, and the system should present a high degree of supramolecular order within bilayers. The transport experiments show that these superstructures form membrane spanning structures with clear cation-conductance behaviors. The macrocycles pointing toward the hydrophylic part of the channel certainly facilitate the transport of the cations, allowing the control of K^+-transport selectivity, which is rarely observed with self-assembled artificial systems. As observed in crystal structures, the dimensional fit of Na^+ cations induce an incomplete coordination ability, which leads, after cation entrance, to a partial dehydration and correspondingly to low transport rate. In contrast, the sandwich-type recognition surrounding the K^+ cations in a similar manner to the water molecules around the hydrated cation in water, has important consequences for the highly selective K^+ translocation along the channel, which totally compensates the energetic cost of their dehydration. Altogether, the present work demonstrates the potential of the investigated channels as an interesting biomimetic alternative of K^+ KcsA channels.

Experimental Section

LUV fabrication: The vesicles (LUVs) were formed using egg yolk L-α-phosphatidylcholine (EYPC chloroform solution, 800 µL, 20 mg) and the appropriate amount of **1a-1b** dissolved in a CHCl$_3$/MeOH mixture. The solution was evaporated without heating and dried overnight under high vacuum. The resulting thin film was hydrated in 400 µL of buffer (10 mM sodium phosphate, pH 6.4, 100 mM NaCl) containing 10 µM HPTS (8-hydroxypyrene-1,3,6-trisulfonic acid trisodium salt). During hydration, the suspension was submitted to eight freeze-thaw cycles (liquid nitrogen, water at room temperature). The obtained white suspension was extruded 21 times through a 0.1 µm polycarbonate membrane, at 35-40°C, in order to transform the large multilamellar liposome suspension (LMVs) into large unilamellar vesicles (LUVs) with an average diameter of 100 nm. The LUVs suspension was separated from extra-vesicular HPTS dye by using size exclusion chromatography (SEC, stationary phase Sephadex G-50, mobile phase: phosphate buffer with 100 mM NaCl), diluted with mobile phase to give 2.8 mL of stock solution. The stock solution has to be used two weeks after its preparation.

Cation transport experiments: We used a ratio data collection method. 100 µL of stock vesicle solution was suspended in 1.88 mL of the corresponding buffer (containing 100 mM of the analyzed cation) and placed into a quartz fluorimetric cell. The emission of HPTS at 510 nm was monitored at two excitation wavelengths (403 and 460 nm) simultaneously. An experiment takes 600 s, with two main events: at 50 s, 29 µL of aqueous NaOH (0.5 M) was added, resulting in a pH increase of about one unit in the extravesicular media. Finally, at 505 s, when the curve is stabilized, the monitoring was stopped by lysing the vesicles with detergent (40 µL of 5% aqueous Triton X-100), in order to equilibrate the intravesicular and the extravesicular solution. The value of transport was obtained as a ratio of the emission intensities monitored at 460 and 403 nm, and normalized to 100% of transport (fluorescence curves are a I/I_0 ratio function on time, between 0 and 1). We calculated the first-order rate constant from the slopes of the plot of ln ($[H^+_{in}]-[H^+_{out}]$) versus time, where $[H^+_{in}]$ and $[H^+_{out}]$ are the intravesicular and extravesicular proton concentrations, respectively. The $[H^+_{out}]$ was assumed to be constant during the experiment (pH 7.4), while $[H^+_{in}]$ values were calculated for each point from the HPTS emission intensity with excitation at 403 nm (using the calibration equation $[H^+_{in}]=1.1684*\log(I/I_0)+6.9807$). Then we determined the fractional

activity (Y), the highest value of I/I_0 before lysing the vesicles with detergent. After considering this value (at 500 s), we expressed Y function on time, and we obtained linear and polynomial fittings. To calculate Hill coefficient, we expressed log of Y versus log of compound concentration. The slope is the Hill coefficient and it is expressing the cooperativity (a Hill coefficient of 1 can be interpreted as cooperative and or higher-order channel formation). See details in the Supporting Information.

Acknowledgements

References

[1] S. M. Hurtley, *Science* **2005,** *310,* 1451-1451.

[2] S. W. Kowalczyk, T. R. Blosser, C. Dekker, *Trends Biotechnol.* **2011,** 29, 607 - 614.

[3] a) F. M. Ashcroft, *Nature* **2006,** 440, 440 - 447; b) R. S. Kass, *J. Clin. Invest.* **2005,**115, 1986-1989.

[4] R. MacKinnon, *Angew. Chem. Int. Ed.* **2004,** 43, 4265 - 4277; *Angew. Chem.* **2004,***116,* 4363-4376.

[5] a) P. Ball, *Nature* **2001,** *409,* 413-416; b) B. Bhushan, *Philos. Trans. R. Soc. A* **2009,** *367,* 1445-1486.

[6] a) N. Busschaert, P. A. Gale, *Angew. Chem. Int. Ed.* **2013,** 52, 1374-1382; *Angew. Chem.* **2013,***125,*1414-1422; b) P. A. Gale, *Acc. Chem. Res.* **2011,** 44, 216-226; c) N. Sakai, S. Matile, *Langmuir* **2013,** 29, 9031-9040.

[7] P. Xin, P. Zhu, P. Su, J. L. Hou, Z. T. Li, *J. Am. Chem. Soc.* **2014,** *136,* 13078-13081.

[8] a) A. Vargas Jentzsch, A. Hennig, J. Mareda, S. Matile, *Acc. Chem. Res.* **2013,** 46, 2791-2800; b) A. V. Jentzsch, D. Emery, J. Mareda, S. K. Nayak, P. Metrangolo, G. Resnati, N. Sakai, S. Matile, *Nat. Commun.* **2012,** 3, 905; c) J. Mareda, S. Matile, *Chem. Eur. J.* **2009,**15, 28-37.

[9] M. S. Kaucher, W. A. Harrell, Jr., J. T. Davis, *J. Am. Chem. Soc.* **2006,***128,* 38-39.

[10]   a) G. W. Gokel, W. M. Leevy, M. E. Weber, *Chem. Rev.* **2004,** *104,* 2723 - 2750; b) G. W. Gokel, K. A. Arnold, M. Delgado, L. Echeverria, V. J. Gatto, D. A. Gustowski, J. Hernandez, A. Kaifer, S. R. Miller, L. Echegoyen, *Pure Appl. Chem.* **1988,** *60*;
c) T. M. Fyles, D. M. Whitfield, *Can. J. Chem.* **1984,**62,507-514;
d) J.-I. Anzai, Y. Suzuki, A. Ueno, T. Osa, *Isr. J. Chem.* **1985,**26, 60-64; e) H. Sakamoto, K. Kimura, Y. Koseki, T. Shono, *J. Chem. Soc. Perkin Trans. 2* **1987,** 1181.

[11]   a) G. W. Gokel, S. Negin, *Acc. Chem. Res.* **2013,** 46, 2824 - 2833; b) G. W. Gokel, *Chem. Commun.* **2000,** 1-9; c) G. W. Gokel, S. Negin, *Adv. Drug Delivery Rev.* **2012,** 64, 784-796.

[12]   a) F. Otis, M. Auger, N. Voyer, *Acc. Chem. Res.* **2013,** 46, 2934-2943; b) A. Lorin, M. Noel, M. E. Provencher, V. Turcotte, C. Masson, S. Cardinal, P. Lague, N. Voyer, M. Auger, *Biochemistry* **2011,** 50, 9409-9420; c) F. Otis, N. Voyer, A. Polidori, B. Pucci, *New J. Chem.* **2006,** 30, 185; d) E. Biron, N. Voyer, J.-C. Meillon, M.-E. Cormier, M. Auger, *Biopolymers* **2000,** 55, 364-372.

[13]   F. Otis, C. Racine-Berthiaume, N. Voyer, *J. Am. Chem. Soc.* **2011,**133, 6481-6483.

[14]   a) Y.-M. Legrand, M. Barboiu, *Chem. Rec.* **2013,** *13,* 524-538; b) A. Cazacu, C. Tong, A. van der Lee, T. M. Fyles, M. Barboiu, *J. Am. Chem. Soc.* **2006,** *128,* 9541-9548; c) M. Barboiu, S. Cerneaux, A. van der Lee, G. Vaughan, J. Am. *Chem. Soc.* **2004,** *126,* 3545-3550.

[15]   a) T. Liu, C. Bao, H. Wang, Y. Lin, H. Jia, L. Zhu, *Chem. Commun.* **2013,** *49,*10311 - 10313; b) T. Liu, C. Bao, H. Wang, L. Fei, R. Yang, Y. Long, L. Zhu, *New J. Chem.* **2014,** *38,* 3507.

[16]   a) R. Newton, *Thorax* **2000,** 55, 603-613; b) S. Fiorucci, A. Mencarelli, G. Palladino, S. Cipriani, *Trends Pharmacol. Sci.* **2009,** 30, 570-580.

[17]   a) Y. Kobuke, T. Nagatani, *Chem. Lett.* **2000,**29, 298-299; b) Y. Zhao, H. Cho, L. Widanapathirana, S. Zhang, *Acc. Chem. Res.* **2013,** *46,* 2763 - 2772; c) Y. Zhao, Z. Zhong, *J. Am. Chem. Soc.* **2005,**127, 17894-17901.

[18]   a) L. Ma, M. Melegari, M. Colombini, J. T. Davis, *J. Am. Chem. Soc.* **2008,** *130,* 2938 - 2939; b) M. Yoshii, M. Yamamura, A. Satake, Y. Kobuke, *Org. Biomol. Chem.* **2004,** 2, 2619 - 2623.

[19]   R. Custelcean, *Chem. Commun.* **2008,** 295.

[20]   a) M. R. Krause, S. L. Regen, *Acc. Chem. Res.* **2014,**47, 35123521; b) H. J. Lee, K. J. Korshavn, A. Kochi, J. S. Derrick, M. H. Lim, *Chem. Soc. Rev.* **2014,** *43,* 6672 - 6682.

[21]   T. Ishi-i, R. Iguchi, E. Snip, M. Ikeda, S. Shinkai, *Langmuir* **2001,** *17,* 5825-5833.

[22]   a) S. Kim, K. Y. Yi, *J. Org. Chem.* **1986,** *51,* 2613-2615; b) Z. H. Sun, M. Albrecht, G. Raabe, F. F. Pan, C. Rauber, *J. Phys. Chem. B* **2015,***119,* 301-306.

[23]   M. Barboiu, Y. Le Duc, A. Gilles, P. A. Cazade, M. Michau, Y.- M. Legrand, A. van der Lee, B. Coasne, P. Parvizi, J. Post, T. Fyles, *Nat. Commun.* **2014,** 5, 4142.

[24]   a) C. J. Haynes, N. Busschaert, I. L. Kirby, J. Herniman, M. E. Light, N. J. Wells, I. Marques, V. Felix, P. A. Gale, *Org. Biomol Chem.* **2014,** 12, 62-72; b) B. A. McNally, A. V. Koulov, B. D. Smith, J. B. Joos, A. P. Davis, *Chem. Commun.* **2005,**1087-1089.

[25]   a) S. Matile, N. Sakai in *Analytical Methods in Supramolecular Chemistry* (Ed.: C. A. Schalley), Wiley-VCH, Weinheim, **2007,** pp. 381-418; b) S. Bhosale, S. Matile, *Chirality* **2006,** *18,* 849856.

[26]   G. Eisenman, R. Horn, *J. Membr. Biol.* **1983,** *76,* 197 - 225.

[27]   a) A. Cazacu, Y. M. Legrand, A. Pasc, G. Nasr, A. Van der Lee, E. Mahon, M. Barboiu, *Proc. Natl. Acad. Sci. USA* **2009,** *106,* 8117-8122; b) M. Barboiu, G. Vaughan, A. van der Lee, *Org. Lett.* **2003,** 5, 3073 - 3076.